DALTON

Relativistic effects in inorganic and organometallic chemistry†

Nikolas Kaltsoyannis*

Department of Chemistry, University College London, 20 Gordon Street, London WC1H 0AJ, UK

Quantum mechanics and the theory of relativity are two of the most important scientific developments of the 20th century. Most of the structure of non-relativistic quantum mechanics was put into place between 1925 and 1927, followed a few years later by Dirac's incorporation of special relativity.[1,2] It is ironic that Dirac himself believed relativistic effects to be 'of no importance in the consideration of atomic and molecular structure and ordinary chemical reactions'.[3] Indeed it was not until the 1970s that the chemical consequences of relativity were fully appreciated.

Since then there has been extensive investigation of the role of relativity in chemistry. It is no coincidence that the emergence of the field parallels the development of computational quantum chemistry, for it is only through the latter technique that we can directly compare non-relativistic atoms and molecules with their relativistic analogues. By now the chemical consequences of relativity are well established, although the point in the Periodic Table at which relativistic effects become important in determining the properties of elements and their compounds is not clear cut; it depends on the property and the definition of important! In the words of Pekka Pyykkö:[4] 'For very precise calculations, relativistic energy contributions are already needed for H_2^+ or H_2. . . . Depending on the accuracy achieved in the calculation, they become relevant again around Cu, or perhaps Ag. For the sixth row (around W to Bi), relativistic effects . . . . provide an explanation for much of the basic freshman chemistry of these elements. For the existing actinoids relativistic effects are essential.'

This contribution begins with a very brief introduction to relativistic quantum mechanics, together with a discussion of its chemical consequences. I have subsequently chosen a number of topics with which to illustrate and highlight these consequences, but it must be emphasised that these topics are not intended to provide an exhaustive coverage. There are several excellent discussions of relativistic effects in chemistry,[4–8] including Pyykkö's comprehensive 1988 review.[4] Most of the material in this article is taken from studies conducted since that review was written, and is specifically chosen with a bias toward inorganic and organometallic chemistry.

Theoretical Overview

The Dirac equation

A comprehensive discussion of relativistic quantum mechanics is not appropriate for an article such as this,‡ although I believe the reader will find some theoretical background helpful in understanding the subsequent topics. We may begin by posing the question, why is the Schrödinger equation incompatible with the theory of relativity? The time-dependent Schrödinger equation for an electron with wavefunction Ψ moving in a general external potential $V(x, y, z)$ is given in (1). Notice that while

$$\left[\frac{-\hbar^2}{2m}\left(\frac{\partial^2}{\partial x^2}+\frac{\partial^2}{\partial y^2}+\frac{\partial^2}{\partial z^2}\right)+V(x,y,z)\right]\Psi = i\hbar\frac{\partial\Psi}{\partial t} \quad (1)$$

there are second-order partial derivatives with respect to the three spatial coordinates x, y and z, there is only a first-order derivative with respect to time. This is at odds with the special theory of relativity, which requires an even-handed treatment of x, y, z and t.

In order to make quantum theory compatible with relativity, Dirac[1–3] suggested an equation of the form (2) to replace the

$$\left[-ic\hbar\left(\alpha_x\frac{\partial}{\partial x}+\alpha_y\frac{\partial}{\partial y}+\alpha_z\frac{\partial}{\partial z}\right)+\beta mc^2+V(x,y,z)\right]\Psi = i\hbar\frac{\partial\Psi}{\partial t} \quad (2)$$

time-dependent Schrödinger equation for electrons, where α_x, α_y, α_z and β are constants and c is the speed of light. The Dirac equation is therefore even-handed in its treatment of space and time, but, in order that it also satisfy other relativistic requirements, α_x, α_y, α_z and β cannot be simple numbers. Instead they are 4×4 matrices, and hence the Dirac equation is meaningful only if the wavefunction Ψ is a four-component column vector (3) where each component, ψ_n, is a function of x, y, z and t.

$$\Psi = \begin{pmatrix}\psi_1\\ \psi_2\\ \psi_3\\ \psi_4\end{pmatrix} \quad (3)$$

In essence, then, there are four solutions to the Dirac equation (four coupled differential equations in the four components of Ψ). They separate into two pairs, one pair with positive energy and the other with negative energy. The positive-energy solutions correspond to a particle of mass m_e and charge $-e$ (*i.e.* an electron) while the negative-energy solutions correspond to a particle of the same mass but with charge $+e$. The Dirac equation therefore predicted the existence of the positron some years before its experimental discovery by Anderson in 1933.[12a] A second triumph of the Dirac equation arises from its prediction that there are *two* positive-energy (electron) solutions. These solutions correspond to the two possible spin states of an electron, and thus the incorporation of relativity into quantum mechanics *via* the Dirac equation leads in a natural way to electron spin, which has to be treated rather clumsily as an 'extra' in non-relativistic quantum mechanics.

The electron solutions to the Dirac equation have ψ_1 and ψ_2 as their principal components; they may be regarded as the Schrödinger equation solutions for up- and down-spin electrons respectively. Components ψ_3 and ψ_4 are radially much more contracted than ψ_1 and ψ_2 and are always very small in the

* E-Mail: n.kaltsoyannis@ucl.ac.uk

† *Non-SI unit employed:* eV ≈ 1.60×10^{-19} J.

‡ For more complete treatments the reader is directed to refs. 4, 7 and 9–11. In addition, a list of 8265 (as of August 1996) references concerning the relativistic treatment of atoms and molecules may be found on the internet at http://www.csc.fi/lul/rtam.

outer regions of an atom. They may, however, become important near the nucleus. The electron density is given by the sum of the squares of all four components of Ψ. In the non-relativistic limit ψ_3 and ψ_4 vanish, thereby recovering the Schrödinger-equation atomic wavefunctions.

The modification of radial atomic wavefunctions and associated eigenvalues

Einstein's special theory of relativity tells us that it is impossible to accelerate a particle to a velocity in excess of that of light. This stems from the relativistic mass increase in equation (4)

$$m = m_0/\sqrt{1 - (v/c)^2} \quad (4)$$

where m is the mass of a particle, of rest mass m_0, moving with velocity v. Clearly, when $v = c$, m becomes infinite.

In atomic units, the average radial velocity, $\langle v_{rad} \rangle$, of the electrons in the 1s shell of an atom is approximately Z, where Z is the atomic number. Thus for gold, for which $Z = 79$, we obtain expression (5) where the speed of light is also expressed in

$$\frac{\langle v_{rad} \rangle}{c} \approx \frac{79}{137} \approx 0.58 \quad (5)$$

atomic units. The average relativistic mass increase of the 1s electron in gold is therefore given by equation (6).

$$m = m_0/\sqrt{1 - (0.58)^2} = 1.23m_0 \quad (6)$$

This has a marked effect on the radial distribution of the electron, as the expression for the Bohr radius has a $1/m$ dependence. Hence the relativistic 1s atomic orbital (AO) of gold has an average radial contraction of *ca.* 20% in comparison with its non-relativistic analogue, an effect that is accompanied by an energetic stabilisation of the electron.

The dependence of relativistic mass corrections on atomic number means that, for light elements, the effects of relativity are generally small. This is clearly not the case for heavy elements, however, and the consequences of relativity for the valence electronic structure of such atoms are often profound (in percentage terms, the modification of the valence-electron radial distributions and energies in heavy elements upon the inclusion of relativity often exceeds that of the core orbitals). Although there are many competing factors that determine the precise valence electronic structure of a heavy element [for a more complete treatment the reader is directed to ref. 12(*b*)], several general trends may be identified. In order that the s functions in higher primary quantum shells remain orthogonal to the core orbitals they are also stabilised by the effects of relativity. This is known as the direct relativistic orbital contraction. Similar, though smaller, effects are experienced by p electrons. In contrast, relativistic valence d and f electrons are *expanded* and *destabilised* with respect to their non-relativistic analogues. This arises from the increased shielding of the nucleus by the outer core s and p electrons of similar radial distribution to the d and f functions, and is known as the indirect relativistic orbital expansion. In very heavy elements such as the actinides the relativistic expansion and destabilisation of the valence f orbitals is sufficient to alter their chemistry markedly in comparison with (hypothetical) non-relativistic analogues.

Relativistically expanded d and f orbitals may themselves have important consequences for (other) valence electrons. If a filled d or f shell lies just inside a valence orbital that orbital may experience an enhanced effective nuclear charge (and hence a contraction/stabilisation) on account of the reduced nuclear screening ability of the d and f electrons. We shall see an example of this effect later in this article in a further discussion of the electronic structure of gold.

Table 1 Energy separations, Δ, of the spin–orbit coupled terms of the ground-state electronic configurations of Cl, I and La. Data from ref. 14

			$\Delta(^2P_{1/2} - {}^2P_{3/2})$		$\Delta(^2D_{5/2} - {}^2D_{3/2})$	
Element	Z	Configuration	cm^{-1}	eV	cm^{-1}	eV
Cl	17	$[Ne]3s^23p^5$	881	0.109		
I	53	$[Kr]4d^{10}5s^25p^5$	7605	0.943		
La	57	$[Xe]5d^16s^2$			1053	0.131

Spin–orbit coupling

One of the principal consequences of the Dirac equation for chemistry stems from its prediction of electron spin. When an electron is part of an atom the magnetic moment associated with its intrinsic spin angular momentum couples with the magnetic field generated by its orbital motion.[13] The resulting states are characterised by non-integral total angular momentum values (j) as a result of the combination of integral orbital angular momentum ($l = 0, 1, 2, 3 \ldots$) with non-integral spin angular momentum ($s = \frac{1}{2}$). Except for s orbitals, for which there is no orbital angular momentum, the spin–orbit interaction splits a shell of given l into subshells with total angular momentum $j = l - \frac{1}{2}$ and $l + \frac{1}{2}$. The factors which govern the magnitude of this spin–orbit splitting in many-electron atoms are complicated but, in general, spin–orbit coupling increases significantly with increasing nuclear charge and, for a given primary quantum shell, decreases in the order p > d > f. This is illustrated by the data in Table 1, which gives the energetic separation of the spin–orbit-coupled terms of the ground electronic configurations of Cl, I and La.

Symmetry and relativistic quantum mechanics: double point groups

The linear combination of atomic orbitals (LCAO) approach to molecular orbital (MO) theory occupies a central position in inorganic chemistry. It is used to rationalise and predict, both qualitatively and quantitatively, the electronic structure and reactivity of molecules ranging from H_2 to transition-metal organometallics. A vital component of this methodology is group theory, and the restrictions placed upon the interaction of AOs within molecules by symmetry are extremely valuable in studies of molecular electronic structure and bonding. The construction of MO energy-level diagrams is carried out by determining the symmetry properties of AOs and combinations of AOs. In doing this, attention is focused exclusively on the *spatial* symmetry of the AOs; electron spin is taken into account only through the use of the Pauli exclusion principle as the resultant MOs are filled with the appropriate number of electrons.

The AOs used in this process are characterised by the orbital angular momentum quantum number, l, which can take only integral values. Hence the construction of MO energy-level schemes in the manner described above involves the determination of the symmetry properties of electronic states characterised by integral angular momentum. We have seen, however, that spin–orbit coupling results in AOs that are characterised by non-integral angular momentum values. Can we still use the same approach to describe/understand the electronic structure of compounds containing atoms for which spin–orbit coupling is significant, *i.e.* are the symmetry properties of non-integral angular momentum states the same as those of integral states?

The answer is that, while we can use the same group theoretical principles as before, we must take account of certain features of the symmetry of non-integral angular momentum states that do not arise in l-based systems. The character of a rotation through an angle α when applied to a state characterised by angular momentum j is given by expression (7). For

$$\chi(\alpha) = \sin\left(j + \frac{1}{2}\right)\alpha \Big/ \sin\left(\frac{\alpha}{2}\right) \quad (7)$$

integral j values we obtain equation (8), *i.e.* rotation by 360°

$$\chi(\alpha + 2\pi) = \chi(\alpha) \quad (8)$$

leaves the system unaltered. However, for states with non-integral j values equation (9) applies, *i.e.* rotation by 360° is not

$$\chi(\alpha + 2\pi) = -\chi(\alpha) \quad (9)$$

an identity operation. We cannot, therefore, treat the symmetry properties of states with non-integral angular momentum (*e.g.* relativistic AOs and MOs formed from them) using normal point groups. Instead we must use extensions to the normal point groups, known as *double groups*.[15,16]

As their name suggests, double groups contain twice as many symmetry operations as normal point groups (known as single groups). In double groups, rotation through 360° is not treated as the identity operation, but as another symmetry operation. It is given the symbol R. The extra operations of the double group are obtained by taking the product of R with all of the operations of the single group, and the double-group identity operation is rotation through 720°.

Double groups contain extra irreducible representations in addition to those of the single group. All integral angular momentum states (*e.g.* non-relativistic, spatial MOs) have symmetry properties which span one or more of the familiar single-group irreducible representations. All states characterised by non-integral angular momentum values (*e.g.* relativistic spin orbitals) have symmetry properties which span one or more of the extra irreducible representations of the double group.

Thus we may use LCAO-MO theory to construct relativistic energy-level diagrams for molecules with one or more heavy atoms, but each of the levels will carry a double-group symmetry label. It is important to note that, while a non-relativistic energy-level scheme consists of spatial MOs into which we may place both up- and down-spin electrons, electron spin is already incorporated in double-point-group symmetry labels. It is therefore conceptually incorrect to represent individual electrons in relativistic MO energy-level diagrams by arrows indicating directions of spin.

The group theoretical relationship between non-relativistic spatial MOs and their relativistic spin–orbital counterparts may be obtained by decomposing the reducible representation created by the direct product of the single-group irreducible representations with that of electron spin. It is frequently found that spin–orbit coupling lifts the degeneracy of single-group irreducible representations, generating additional energy levels. This is of critical importance in the interpretation of the electronic spectra of compounds containing heavy elements; single-group treatments fail to reproduce the spectra even qualitatively. We shall see examples of the use of double point groups later in this article.

Computational techniques

As I have already stated, by far the largest area of research to focus on the chemical consequences of relativitity is computational quantum chemistry. This section therefore provides a very brief overview of the most popular and successful methodologies. A more comprehensive account may be found in the excellent review by Pepper and Bursten.[8]

In general we may separate the methods for incorporating relativistic effects into molecular electronic structure calculations into two areas. The first approach is based upon the Pauli approximation,[7,11] which divides relativistic effects into different categories and adds terms for each of these onto the non-relativistic Schrödinger Hamiltonian. In most cases, computational methods employing the Pauli Hamiltonian account only for the relativistic modification of AO energies. Spin–orbit coupling is not explicitly included and the calculated MOs are bases for the irreducible representations of the molecular single-point groups. This method has the advantage of straightforward comparison with non-relativistic calculations. The relativistic extended-Hückel (REX) method of Lohr and Pyykkö,[17] the quasi-relativistic scattered wave Xα (QRSW-Xα)[18,19] and discrete variational[20] (DV) implementations of density functional theory (DFT) and the Hay–Wadt–Kahn effective core potentials[21] (ECPs) for use in *ab initio* Hartree–Fock (HF) calculations are examples of this type of approach.

The use of ECPs (both relativistic and non-relativistic) in *ab initio* calculations (and in some DFT codes) is so widespread as to merit additional comment. The difficulty in solving such calculations rises very rapidly with the number of electrons. Hence the core-electron wavefunctions are frequently replaced with an ECP, thereby reducing the calculation to a more computationally feasible valence-electron problem.* Such an approach has proved highly successful, and is virtually mandatory when performing *ab initio* calculations on transition-metal and f-element compounds.

The second type of relativistic molecular electronic structure calculations involves the solution of the full Dirac equation. Spin–orbit coupling is therefore treated directly in this approach, and the calculated orbitals are bases for the irreducible representations of the molecular double-point group. The Dirac–Fock–Slater (DFS) DV DFT approach of Ellis[22,23] and Pitzer's relativistic ECPs[24] are examples of this methodology.

We shall come across examples of the various types of calculational approach throughout this article. As computational chemistry is riddled with acronyms, Table 2 provides definitions of those employed herein.

Table 2 Definitions of the computational chemistry acronyms used

Acronym	Definition
REX	Relativistic extended Hückel
QRSW-Xα	Quasi-relativistic scattered wave Xα
DV-Xα	Discrete variational Xα
DFT	Density functional theory
ECP	Effective core potential
HF	Hartree–Fock
DF	Dirac–Fock
HFS	Hartree–Fock–Slater
DFS	Dirac–Fock–Slater
MP	Møller–Plesset

Gold: a 'Relativistic' Element

The elements of the third transition and 6p series frequently exhibit strong relativistic effects in their chemistries. There has been much work, for example, on the role of relativity in the chemistry of mercury.[25–28] However, a maximum of relativistic effects has been identified at gold,[4] and I have therefore chosen this element to illustrate some of the chemical consequences of relativity. I shall begin by discussing how the atomic properties of gold are affected by relativity, before moving on to describe two aspects of the chemistry of gold in which relativity plays a significant role.

* In addition to the elimination of the core electrons, the benefits of ECPs include the elimination of the corresponding 'sharp' basis functions and the ability to include relativistic phase shifts in the potential, thereby leaving non-relativistic dynamics for the valence part (where electron velocities are small).

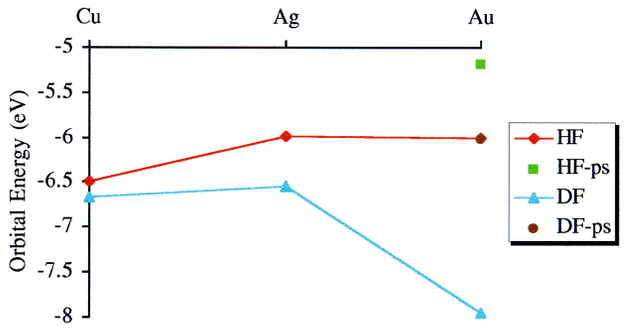

Fig. 1 Calculated [Hartree–Fock (HF) and Dirac–Fock (DF)] valence s-orbital energies for Cu, Ag and Au; 'ps' indicates pseudo-gold without the 4f electrons. Data from refs. 32 and 33. Note that the trend in the negative of the experimental [34] first ionisation energies (7.726, 7.756 and 9.255 eV respectively) closely mirrors the relativistic DF s-orbital energies

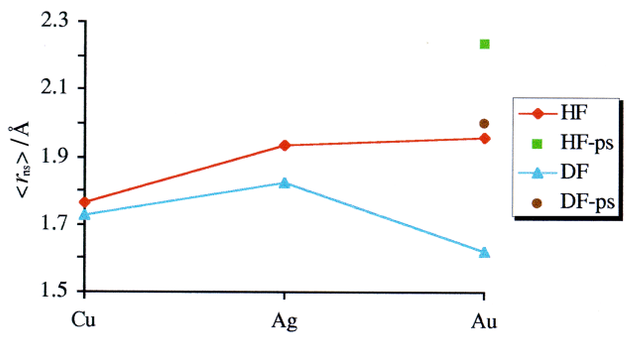

Fig. 2 Calculated $\langle r_{ns} \rangle$ expectation values for Cu ($n = 4$), Ag ($n = 5$) and Au ($n = 6$); 'ps' as in Fig. 1. Data from refs. 32 and 33

Atomic effects: relativity and the lanthanide contraction

It is well known that third-row transition-metal atoms are of similar size to their second-row counterparts. For example, silver and gold both have a metallic radius of *ca.* 1.44 Å,[29] and a recent comparison of the crystal structures of bis(trimesitylphosphine)gold(I) and bis(trimesitylphosphine)silver(I) tetrafluoroborate has confirmed theoretical predictions that the covalent radius of gold (1.25 Å) is actually *less* than that of silver (1.33 Å).[30] This is termed the lanthanide contraction, and is usually attributed to the effect of the 4f electrons on the effective nuclear charge, Z^*, experienced by the valence electrons. The 14 4f electrons do a poor job of screening the corresponding 14 units of nuclear charge, with the result that Z^* for the valence electrons of the third-row transition metals is higher than if the core electrons were exclusively s, p and d.

The above reasoning relies entirely on shell-structure arguments. However, a number of authors [4,31,32] have posed the question, is the lanthanide contraction solely a result of shell-structure effects or is relativity a factor? Comparative non-relativistic Hartree–Fock and relativistic Dirac–Fock (DF) calculations have been performed for all the elements,[33] together with calculations on pseudo-atoms in which the f electrons have been removed (and hence the nuclear charge reduced by 14).[31,32] Some of the results are presented in Figs. 1 and 2, which show the *n*s ($n = 4$–6) orbital energies and $\langle r_{ns} \rangle$ expectation values respectively for Cu, Ag and Au.

These fascinating data reveal a complicated interplay of relativistic and shell-structure effects. The first point to note is how the relativistic calculations indicate a more stable and contracted *n*s AO than do their non-relativistic counterparts (compare DF with HF), with the most pronounced effect at gold. Secondly, notice that the non-relativistic HF calculations find a more stable and contracted gold 6s AO than in pseudo-gold (HF-ps). This is clear evidence for the 4f shell-structure effect. Furthermore, the DF calculations reveal that the marked relativistic stabilisation and contraction of the 6s AO occurs only when the 4f shell is included; relativistic pseudo-gold (DF-ps) has a 6s electron with similar energy and radial expansion to that of non-relativistic gold. The conclusion from these data is therefore that the relativistic stabilisation and contraction of the 6s AO in gold is *not* a direct relativistic effect (*i.e.* not the result of the stabilisation of the core s electrons permeating up through the primary quantum shells), but is attributable (at least in part, see below) to the 4f electrons.

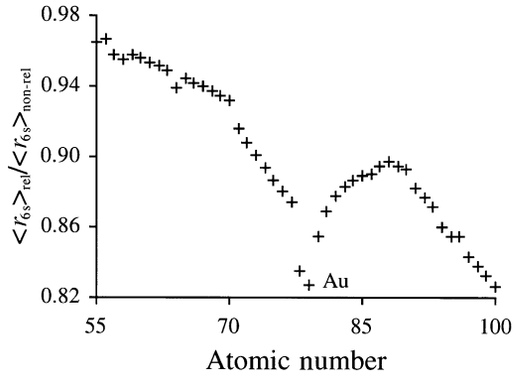

Fig. 3 The relativistic contraction of the 6s shell of elements Cs to Fm, calculated as $\langle r_{6s} \rangle_{rel} / \langle r_{6s} \rangle_{non\text{-}rel}$. Data from ref. 33. After Pyykkö[4]

Is this evidence that the lanthanide contraction is purely a shell-structure effect? Certainly not! The relativistic 4f electrons experience a significant expansion in comparison with their non-relativistic analogues (the indirect relativistic orbital expansion referred to earlier) and are thus even poorer at screening the additional nuclear charge. We may therefore conclude that the lanthanide contraction is a result of both shell-structure and relativistic effects; the indirect relativistic orbital expansion of the 4f electrons reduces their screening ability and therefore increases the effective nuclear charge experienced by the valence electrons.

As the third transition series is crossed the 4f electrons become increasingly core-like. Other workers have examined the origin of the 'gold maximum' and have concluded that, as far as the relativistic contraction of the 6s AO is concerned, the 5d electrons play at least as big a role as the 4f.[12] The mechanism by which the 5d AOs affect the 6s, however, is the same as that discussed above for the 4f, *i.e.* the relativistic expansion of the 5d electrons increases the effective nuclear charge experienced by the 6s. It would therefore appear that the relativistic contraction of the 6s AO of gold arises from a relativistically enhanced reduction in the nuclear screening ability of *both* the 4f and the 5d electrons.

In order to place the relativistic contraction of the 6s AO of gold in context, it is instructive to compare the non-relativistic and relativistic expectation values for r_{6s} for the elements Cs ($Z = 55$) to Fm ($Z = 100$). This is shown in Fig. 3, which plots $\langle r_{6s} \rangle_{rel} / \langle r_{6s} \rangle_{non\text{-}rel}$ for elements 55–100. It may be seen that there is a pronounced maximum of the contraction at gold; not until fermium (element 100) is reached is an equally strong contraction observed.

Before leaving these purely atomic effects, it is worth comparing the non-relativistic and relativistic orbital energies of the $(n - 1)$d and *n*s electrons of Ag and Au (Fig. 4). The relativistic stabilisation of the 6s AO of gold is once again evident, together with the concomitant destabilisation of the 5d AOs. Both of these effects are much less pronounced in silver, with the result that the energetic separation of the valence d and s shells of Au is significantly smaller than that in Ag. The most striking consequence of this is the colour of gold. Fine gold has an absorption beginning at 2.4 eV, attributed to a transition from the filled 5d band to the Fermi level (essentially the 6s band).[36] It therefore reflects red and yellow light and strongly

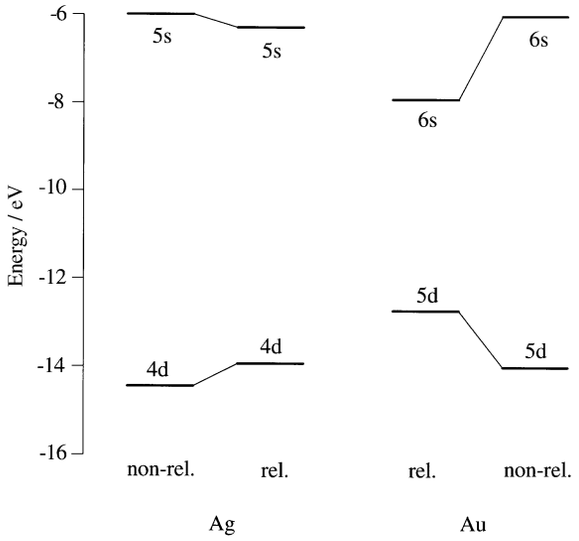

Fig. 4 Calculated non-relativistic and relativistic ($n - 1$)d and ns orbital energies for Ag ($n = 5$) and Au ($n = 6$). Relativistic d-orbital energies are the weighted average of the $d_{\frac{3}{2}}$ and $d_{\frac{5}{2}}$ spin–orbit components. Data from ref. 33. After Pyykkö[35]

absorbs blue and violet. The analogous absorption for silver, however, lies in the ultraviolet, at around 3.7 eV. The difference arises from the larger relativistic modification of the valence d and s orbital energies for gold. Non-relativistic gold would be white, like silver, on account of the bigger band gap.

Relativistic bond-length contractions

A marked reduction in the lengths of covalent bonds involving gold atoms is often found on moving from non-relativistic to relativistic calculations. In a density functional study of MCH_2^+ (M = Ni, Pd, Pt, Ir or Au), Heinemann *et al.*[37] calculated a non-relativistic Au–C distance of 2.153 *vs.* 1.867 Å relativistically. The DFS calculations on Au_2 find a 0.206 Å shortening of the Au–Au bond *vs.* equivalent non-relativistic Hartree–Fock–Slater (HFS) calculations.[38] Furthermore, relativistic calculations consistently predict shorter gold covalent bond lengths than equivalent calculations on silver compounds. Table 3 presents M–C bond lengths in MCH_3, MC_6H_5 and $M(CH_3)_2^-$ for M = Cu, Ag and Au.[39] The calculated Au–C distances in $AuCH_3$ and AuC_6H_5 are approximately 0.1 Å shorter than in the silver analogues.

The reader may be forgiven for concluding that the relativistic contraction in bond lengths is a direct consequence of the AO contraction, on the basis that in order to achieve the most efficient overlap of the contracted AOs the nuclei have to be closer together. Indeed this was assumed to be the case[6] until the work of Ziegler, Snijders, Baerends and Pyykkö[41–43] produced the (initially surprising) result that the two effects are largely unrelated. It was found that the bond-length contractions could be reproduced by applying first-order perturbation theory to the non-relativistic, uncontracted AOs. This approach (which is an example of the Pauli approximation referred to in the section **Computational techniques**) indicates that the bond-length contractions arise from the effect of the relativistic modifications to the Hamiltonian energy operator when applied to the non-relativistic AOs. These relativistic modifications reduce the kinetic energy increase experienced by the electrons as the atoms are pushed together, causing the minima in the binding-energy curves to shift to smaller internuclear distances. The relativistic AO contraction and that of bond lengths are therefore two parallel but largely independent effects.

The data in Table 3 indicate that relativistic bond-length contractions are also significant for Cu, with a 0.057 Å Cu–C shortening in $CuCH_3$ on moving from a non-relativistic to a relativistic ECP. In order to test this conclusion further, the authors calculated the Cu–C bond length in $Cu(CH_3)_2^-$ and compared the results with experiment. It may be seen that the calculation with the relativistic ECP is closer to the experimental bond length than that with the non-relativistic ECP.

Table 3 The M–C bond lengths (Å) in MCH_3, MC_6H_5 and $M(CH_3)_2^-$ (M = Cu, Ag or Au). Data from ref. 38. All calculations are *ab initio* (with non-relativistic or relativistic ECPs) and include electron correlation at the MP2[40] level

M		MCH_3	MC_6H_5	$M(CH_3)^{2-}$
Cu	Relativistic calculation	1.866	1.850	1.922
	Non-relativistic calculation	1.923		1.963
	Experimental			1.935
Ag	Relativistic calculation	2.111	2.091	
Au	Relativistic calculation	2.017	1.981	

Table 4 The Au–Se–Au angle (°) in $(H_3PAu)_2Se$. Data from ref. 46

	Non-relativistic ECP	Relativistic ECP	
Hartree–Fock (uncorrelated)	111.9	97.8	
Hartree–Fock + MP2 (correlated)	87.3	75.4	
Experimental			79.1

The 'aurophilicity' of Au^I

Closed-shell metal cations such as Au^I ([Xe]$4f^{14}5d^{10}$) would normally be expected to repel one another. By the end of the 1980s, however, there was sufficient crystallographic evidence of *attractions* between gold(I) cations to lead Schmidbaur to coin the phrase 'aurophilic attraction' or 'aurophilicity'.[44,45] Given that so much of gold chemistry is influenced by relativity, it was natural to inquire as to whether the aurophilic attraction is also a relativistic effect. Görling *et al.*[46] used Ellis' DV-Xα density functional method to study the electronic structure of a fascinating series of gold cluster compounds, the main-group-element-centred octahedral complexes $[\{(H_3P)Au\}_6X_m]^{m+}$ (X_1 = B, X_2 = C, X_3 = N). These compounds, which may be formally regarded as containing gold(I) cations, feature quite short, 'aurophilic' Au–Au distances. Much of the study focused on the role of the gold 5d AOs in Au–Au bonding. d-Orbital participation can, of course, be achieved only if the formal d^{10} configuration is broken, *e.g.* through 6s/5d hybridisation. The conclusion was that there is a prominent contribution of the gold 5d AOs to the Au–Au bonding within the cluster, *via* 6s/$5d_{z^2}$ hybridisation in the MOs of a_{1g} symmetry. Furthermore, it was argued that the effect has its origin in the relativistic modification of the gold valence AO energies, which brings the 5d and 6s orbitals into close energetic proximity (Fig. 4).

Pyykkö and Li[47,48] also investigated the origin of the aurophilic attraction, but came to very different conclusions. They argued that the effect is primarily due to electron correlation and not s–d hybridisation. Table 4 gives calculated[47] and experimental Au–Se–Au angles in structure **1**. Pyykkö and Li maintain that, if hybridisation effects are important, the Au···Au attraction (as evidenced by the small Au–Se–Au angle) should be present in the uncorrelated calculations. Their data show that the experimental Au–Se–Au angle is reproduced closely only when a relativistic ECP is employed for Au *and* electron correlation is included [*via* Møller–Plesset (MP) theory[40]]. The uncorrelated Au–Se–Au angle, even with a relativistic ECP, is still 18.7° larger than the experimental value.

Further support for this conclusion came from their study[48] of the Au–Au potential curves in structure **2**. For a wide range of X all of the Au–Au potential curves are calculated to be repulsive at the HF (uncorrelated) level. This stands in marked

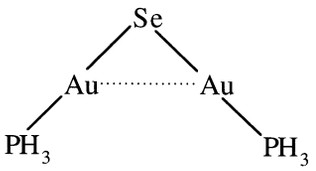

1

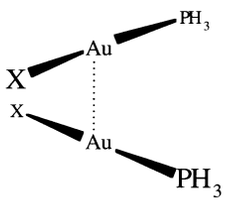

2

contrast to the equivalent curves at the HF + MP2 level, all of which are now attractive with well depths ranging from 12.3 kJ mol^{-1} for X = F to 25.1 kJ mol^{-1} for X = SCH_3. Once again, therefore, the aurophilic attraction is reproduced theoretically only upon the inclusion of electron correlation.

Häberlein *et al.*[49] revisited the octahedral gold clusters $[(LAu)_6X]^{m+}$ (X = B, $m = 1$; X = C, $m = 2$; X = N, $m = 3$; L = PH_3 or PMe_3) in a more extensive study probing the effects of the charge on the cluster cations, the structural consequences of an atom in the centre of the cluster and the extent of relativistic and electron-correlation effects. Among their conclusions were: (*a*) the bonding in element-centred gold clusters is mainly radial, between the gold phosphine units and the central atom; (*b*) although it is not easy to isolate the effects of electron correlation in a density functional study, meaningful electronic structure investigations of gold cluster compounds have to include some treatment of correlation effects and (*c*) relativity and the interaction of gold with the phosphine ligands combine to produce an effective gold electronic configuration closer to $5d^9$ than $5d^{10}$.

Thus the origin of the aurophilic attraction has not yet been uniquely and unambiguously established. It is not clear if this is due to intrinsic differences in the Au–Au interactions in the different molecules under investigation, or to the philosophically different theoretical methods used to study them. The debate continues.

Electronic Structure of $[M(\eta^5\text{-}C_5H_5)_3]$ (M = f element)

The organometallic chemistry of the f elements, while later in starting than that of the transition metals, is now well established. The lanthanide series has an extensive organometallic chemistry and, while that of the actinides is largely focused (for reasons of radioactivity and availability) on Th and U, many organoactinide compounds are also known. As with other f-element compounds, the extent to which relativity affects the metal–ligand interactions in organo-lanthanide and -actinide molecules is of great interest, particularly in relation to the role of the metals' valence d and f orbitals. I have chosen one of the most widely studied f-element organometallic systems, $[M(\eta^5\text{-}C_5H_5)_3]$, to illustrate the methods employed in probing the metal–ligand interactions and the conclusions drawn from those investigations. The high symmetry of these elegant molecules allows the respective roles of the metal valence AOs to be isolated.

The compound $[M(\eta^5\text{-}C_5H_5)_3]$, in which the metal atom and the $\eta^5\text{-}C_5H_5$ centroids are coplanar, is a common structural motif among the f elements. Its electronic structure has been investigated by a number of workers,[50–59] not only because of the intrinsic interest in the metal–ligand interactions, but also because there are almost no transition-metal compounds containing three $\eta^5\text{-}C_5H_5$ ligands (either as the entire ligand environment or in conjunction with other groups). This may be explained with reference to Fig. 5, an energy-level diagram of the calculated[59] (DV-Xα) valence MOs of $[M(\eta^5\text{-}C_5H_5)_3]$ (M = Ce or Th). The principal metal–$(\eta^5\text{-}C_5H_5)$ bonding in $[M(\eta^5\text{-}C_5H_5)_3]$ occurs between the valence AOs of the central metal and the highest occupied molecular orbitals (HOMOs) of the $\eta^5\text{-}C_5H_5$ ligands. These are C $2p_\pi$ MOs and, as they have two nodal planes in addition to the plane of the carbocyclic skeleton, are referred to as the π_2 orbitals. When three $\eta^5\text{-}C_5H_5$ units combine to form a C_{3v} ligand field their π_2 orbitals produce $a_1 + a_2 + e + e$ levels, with the a_2 orbital being significantly destabilised above the other combinations owing to ligand–ligand interactions. These orbitals are labelled $(\eta^5\text{-}C_5H_5)$ π_2 on the left-hand side of Fig. 5(*a*) and 5(*b*). The scarcity of the $[M(\eta^5\text{-}C_5H_5)_3]$ unit for transition metals and the abundance of the same unit among the f elements may be traced to the a_2 level generated by the three $\eta^5\text{-}C_5H_5$ ligands. There is no d orbital that transforms as a_2 symmetry in C_{3v} ligand environments; in contrast the $f_{y(3x^2-y^2)}$ orbital can stabilise the ligand a_2 combination and provide significant metal–ligand bonding in the process.

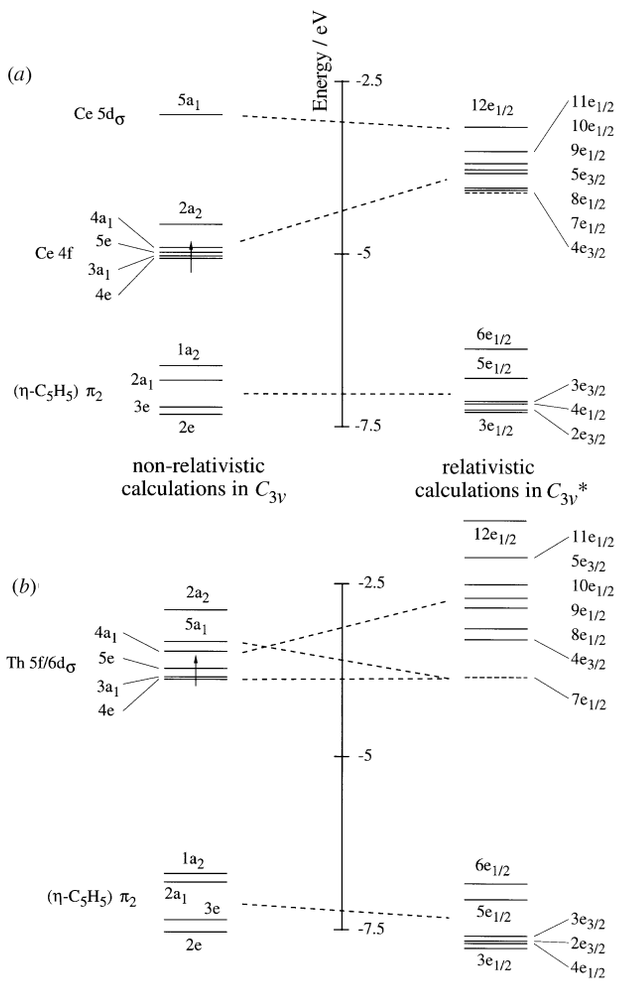

Fig. 5 Calculated non-relativistic and relativistic molecular orbital energy levels of $[M(\eta^5\text{-}C_5H_5)_3]$ [M = Ce (*a*) or Th (*b*)]. Relativistic molecular orbital symmetry labels belong to the C_{3v}* double-point group. Dashed lines across the energy scales indicate broadly how the non-relativistic molecular orbitals relate to the relativistic. The highest occupied orbitals of the relativistic calculations are indicated by a dashed horizontal line. Data from ref. 59

Bursten and Strittmatter[52–56] have used the QRSW-Xα implementation of DFT in an extensive computational study of

the bonding in $[M(\eta^5\text{-}C_5H_5)_3]$ (M = Ln or An) and derivative molecules. They concluded that, in the case of $[An(\eta^5\text{-}C_5H_5)_3]$, the actinide 6d AOs are more important than the 5f in bonding the ligands to the metal on account of the greater radial extension of the 6d orbitals *vs.* the 5f. In $[Ln(\eta^5\text{-}C_5H_5)_3]$ the 5d AOs of the Ln atoms have a similar function to their actinide 6d counterparts, but the lanthanide 4f AOs do not interact with the ligands to the same extent as do the actinide 5f. This is attributed to the differences in radial extension and energies of the two sets of orbitals.[56]

These conclusions are supported by a combined theoretical and experimental study of bis(polymethylcyclopentadienyl)-lanthanide hydrocarbyl compounds (Ln = La, Ce, Nd, Sm or Lu).[60] Non-relativistic DV-Xα and *ab initio* (with relativistic ECPs) calculations, in conjunction with gas-phase ultraviolet photoelectron spectroscopy (PES), were used to establish that, while the lanthanide 5d AOs participate significantly in metal–ligand bonding, the 4f contribution is negligible. It was also found that a gradual stabilisation of the 4f AOs occurs as the lanthanide series is crossed, to the extent that they are almost core-like in $[Me_2Si(\eta^5\text{-}C_5Me_4)_2Lu\{CH(SiMe_3)_2\}]$.

Bursten and Strittmatter[57,61] found a similar stabilisation of the actinide 5f-based MO manifold in $[An(\eta^5\text{-}C_5H_5)_3]$ as the actinide series is crossed. At the start of the actinide period the 5f manifold is less stable than the $6d_\sigma$ MO (largely actinide $6d_{z2}$), but is rapidly stabilised with increasing atomic number. Thus while $[U(\eta^5\text{-}C_5H_5)_3]$, $[Np(\eta^5\text{-}C_5H_5)_3]$ and $[Pu(\eta^5\text{-}C_5H_5)_3]$ are calculated to have the formal electronic configurations $6d^05f^3$, $6d^05f^4$ and $6d^05f^5$ respectively, $[Pa(\eta^5\text{-}C_5H_5)_3]$ is predicted to be $6d^15f^1$ and $[Th(\eta^5\text{-}C_5H_5)_3]$ $6d^15f^0$. This is in agreement with experimental conclusions on the closely related $[Th\{\eta^5\text{-}C_5H_3(SiMe_3)_2\text{-}1,3\}_3]$.[62,63] The crossing of the 6d and 5f levels at Pa has also been observed in REX[64] and HFS[65] studies of the actinocenes, $[An(\eta^8\text{-}C_8H_8)_2]$.

As part of a project to reproduce computationally the electronic absorption spectra of a range of 'f^1' compounds (f-element molecules in which the metal is in an oxidation state one less than its group valence), Kaltsoyannis and Bursten[59] used a fully relativistic implementation of the DV-Xα methodology to study $[Ce(\eta^5\text{-}C_5H_5)_3]$ and $[Th(\eta^5\text{-}C_5H_5)_3]$. Some of the results of this investigation are presented pictorially in Fig. 5. Focusing on $[Ce(\eta^5\text{-}C_5H_5)_3]$ [Fig. 5(*a*)], it may be seen that the non-relativistic calculation predicts a formal $4f^1$ configuration (the HOMO is the 4f-based 4e level). Above the 4f manifold ($4e–2a_2$) comes the $5a_1$ cerium $5d_{z^2}$-based orbital. The 4f manifold is destabilised on the incorporation of relativity [the relativistic calculational results are shown on the right-hand side of Fig. 5(*a*)] although the effect is not sufficient to alter the formal ground-state electronic configuration.

This stands in marked contrast to the equivalent calculations on $[Th(\eta^5\text{-}C_5H_5)_3]$. At the non-relativistic level, $[Th(\eta^5\text{-}C_5H_5)_3]$ is similar to $[Ce(\eta^5\text{-}C_5H_5)_3]$, with a formal $5f^1$ ground-state configuration. The inclusion of relativity, however, produces a $7e_{1/2}$ HOMO which contains predominant thorium $6d_{z^2}$ (in non-relativistic notation) character, *i.e.* a formal $6d^1$ configuration. Thus both the quasi-relativistic SW-Xα and the fully relativistic DV-Xα computational methods agree that the ground-state configuration of $[Th(\eta^5\text{-}C_5H_5)_3]$ is formally $6d^1$. Furthermore, the DV-Xα results indicate that this is a direct result of the effects of relativity.

The consequences of this unusual electronic configuration for the electronic absorption spectrum of $[Th(\eta^5\text{-}C_5H_5)_3]$ are profound. Non-relativistically $[Th(\eta^5\text{-}C_5H_5)_3]$ is predicted to give rise to weak f ⟶ f/d optical transitions, whereas the relativistic calculation suggests a spectrum consisting of d ⟶ f promotions. The intense absorptions seen in the experimental electronic absorption spectrum of $[Th\{\eta^5\text{-}C_5H_3(SiMe_3)_2\text{-}1,3\}_3]$[62,63] are attributed to promotion of the single 6d electron into the 5f manifold, in agreement with the relativistic calculation.

The Dewar–Chatt–Duncanson Model of Synergic Bonding

The bonding of ligands such as CO and phosphines to transition metals is usually rationalised using the Dewar–Chatt–Duncanson (DCD) approach.[66,67] This suggests that there are two synergic processes occurring; donation of electron density from a ligand orbital of σ symmetry with respect to the metal–ligand axis into an empty metal d orbital, with simultaneous donation of electron density from a filled metal d_π orbital into an empty π* orbital on the ligand. This model has recently been the subject of a number of computational investigations, with the effects of relativity coming under particular scrutiny. Li *et al.*[68] used non-relativistic and relativistic density functional theory to study $[M(CO)_4]$ (M = Ni, Pd or Pt), $[M(CO)_5]$ (M = Fe, Ru or Os) and $[M(CO)_6]$ (M = Cu, Mo or W). Among their findings was a significant increase in the M–CO bond strength in the third-row compounds on comparison of the relativistic calculations with the non-relativistic analogues. This increase, which is substantially greater than in the 3d and 4d congeners, ranged from 20.9 kJ mol^{-1} in $[W(CO)_6]$ to 47.2 kJ mol^{-1} in $[Pt(CO)_4]$, a trend which reflects one of their general conclusions; relativistic effects increase in the order $[W(CO)_6] < [Os(CO)_5] < [Pt(CO)_4]$.

The origin of the relativistic increase in M–CO bond strengths may be traced to the relativistic modification of AO energies. In particular, the destabilisation of the metals' 5d AOs brings them into closer energetic proximity with the vacant CO π* MOs, thereby increasing the $d_\pi \rightarrow$CO π* back donation. This increase was found to be the predominant stabilising contribution to the M–CO bond energies in all cases.

The σ-donation component of the synergic bond is also affected by relativity. In the case of $[W(CO)_6]$ and $[Os(CO)_5]$, σ donation CO ⟶ M is into metal-based orbitals of $5d_\sigma$ and $6p_\sigma$ character respectively. Both of these sets of MOs are destabilised slightly by relativity, and σ donation decreases. In contrast, σ donation CO ⟶ Pt in $[Pt(CO)_4]$ is into Pt-based MOs with appreciable metal 6s character. These are stabilised on the incorporation of relativistic effects and hence σ donation increases. Thus for $[Pt(CO)_4]$ relativity increases both the σ and π components of the synergic bond.

The relative strengths of σ donation and π back donation in transition-metal carbonyl complexes has been studied by Dapprich and Frenking.[69] They employed the charge-decomposition method to analyse the results of HF + MP2 (with relativistic ECPs) calculations of $[W(CO)_6]$ and $[M(CO)]^+$ (M = Ag or Au). They found that in $[W(CO)_6]$, σ donation and π back donation are of similar magnitude, in contrast to $[M(CO)]^+$ for which π back donation is virtually negligible and σ donation from CO to metal dominates.

Li *et al.*[70] have also carried out a density functional study of the bonding of the X_2 ligand to the metal centre in $[M(PH_3)_2X_2]$ (M = Ni, Pd or Pt; $X_2 = O_2$, C_2H_4 or C_2H_2) and $[M(CO)_4X_2]$ (M = Fe, Ru or Os; $X_2 = C_2H_4$). In all cases the relativistic M–X_2 bond strengths display a V-like trend from top to bottom within a triad, with the minimum at the second row. The cause of the increase in M–X_2 bond strength between second and third row was again attributed to relativistically enhanced π back donation. A concomitant distortion of the X_2 ligand was found in the calculated molecular geometries; an increase in O–O or C–C bond lengths and a bending of the H atoms (in C_2H_4 and C_2H_2) away from the metal. Both of these effects are consistent with a reduction in π bonding within the X_2 ligand.

The nature of the π-acceptor orbitals in phosphine ligands has been the subject of investigation.[71–73] Xiao *et al.*[70] argued that, rather than the traditional phosphorus 3d AOs, P–R (or P–X) σ* MOs of π symmetry with respect to the metal–ligand axis are the principal acceptors of metal d_π electron density. Recently Fantucci *et al.*[74] found that, in a combined relativistic

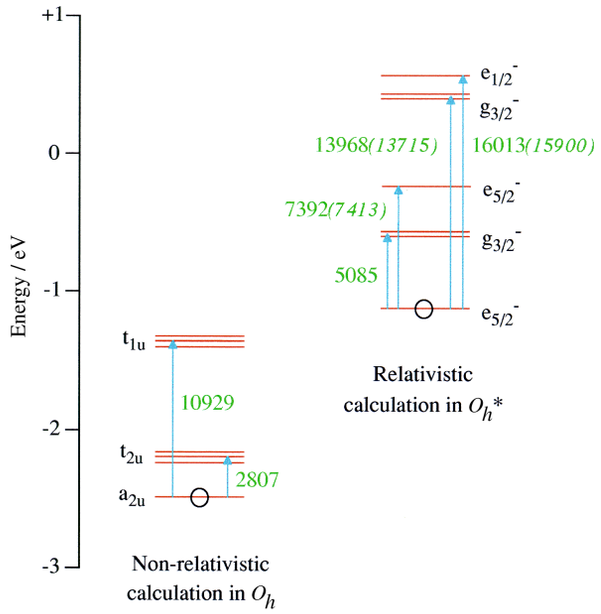

Fig. 6 Calculated non-relativistic and relativistic uranium 5f-based molecular orbital energy levels of UF_6^-. The transitions of the single 5f-based electron (represented by a circle) from the a_{2u} (non-relativistic) and $e_{5/2}^-$ (relativistic) highest occupied orbitals to the other 5f-based levels are represented by vertical arrows. The wavenumbers of the transitions are shown in green as calculated (*experimental*). Relativistic molecular orbital symmetry labels belong to the O_h* double-point group. Data from ref. 76

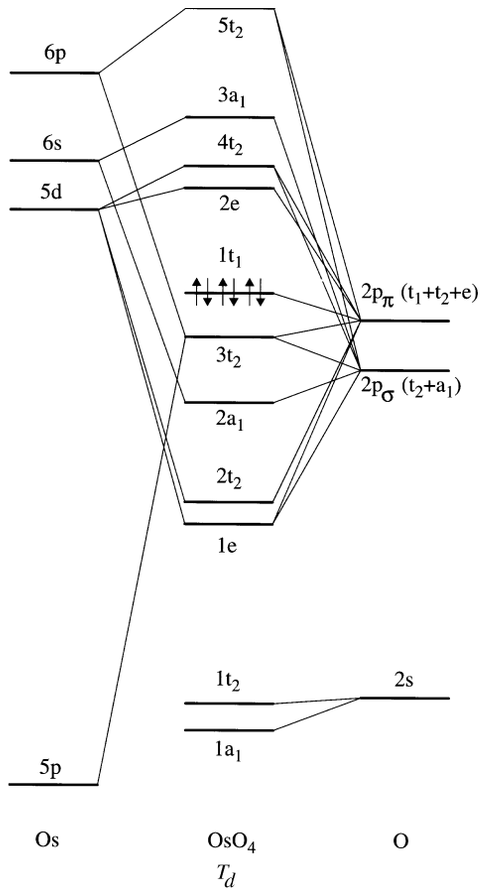

Fig. 7 Qualitative molecular orbital energy-level diagram for OsO_4. Symmetry labels in parentheses are those of the orbitals of an O_4 tetrahedron

density functional and *ab initio* study of $[Pt(PX_3)_2]$ (X = H or F), the accumulation of electronic charge in the MOs derived from the phosphorus 3d AOs was between 50 and 60% of the total π-electron density transferred from Pt to PX_3. This suggests that these 3d AOs play at least as important a role as the PX_3 σ* MOs in the π component of the synergic bond. However, Fantucci *et al.* sounded a note of caution as they also found that charge is accumulated in the phosphorus σ-donor orbitals on complexation, completely counter to the DCD mechanism. They concluded that the phosphorus AO populations cannot be related solely to Pt ⟷ PX_3 charge exchange, but are also affected by charge rearrangements internal to the ligand.

Spin–Orbit Coupling and Electronic Spectroscopy

Thus far the topics that I have chosen have been primarily concerned with the chemical consequences of the relativistic modification of AO energies. In this section I shall explore the second major effect of relativity, spin–orbit coupling. Spin–orbit effects are arguably most important in the area of electronic spectroscopy, and hence this section concentrates upon two examples drawn from this field.

Optical spectra of AnX_6^{q-}

If a transition-metal atom or ion with a formal d^1 configuration is placed in an octahedral ligand field a band is likely to be observed in the optical spectrum corresponding to the promotion of the single metal d electron from the t_{2g} orbitals to the vacant e_g levels. In $[Ti(H_2O)_6]^{3+}$, for example, this transition occurs at *ca.* 20 000 cm^{-1}.[75] Any asymmetry in the shape of the band is likely to be due to, for example, vibronic coupling and/or the Jahn–Teller effect. Spin–orbit coupling can be safely ignored (at least for the 3d and 4d metals).

However, the role of spin–orbit coupling in the electronic structure of actinide complexes is much greater. This may be illustrated with reference to octahedral actinide complexes with the metal in a formal oxidation state one less than its group valence, *i.e.* $5f^1$ systems. The effect of the octahedral ligand field on the metal's 5f orbitals is to split them into a lowest-lying a_{2u} level, an intermediate t_{2u} set and a least-stable t_{1u} orbital. We might therefore expect two electronic bands in the optical spectrum, corresponding to the promotions $a_{2u}^1t_{2u}^0t_{1u}^0 \longrightarrow a_{2u}^0t_{2u}^1t_{1u}^0$ and $a_{2u}^1t_{2u}^0t_{1u}^0 \longrightarrow a_{2u}^0t_{2u}^0t_{1u}^1$. This situation is illustrated in Fig. 6, which shows the calculated[76] ground-state energies of the 5f-based MOs of UF_6^-, together with the energies of the transitions (in wavenumbers; plain green text) of the single 5f electron within the 5f manifold. Two separate studies have been performed, one using non-relativistic DFT and the other employing fully relativistic DFT. Notice how there are twice as many relativistic electronic transitions as non-relativistic ones. This arises from the effects of spin–orbit coupling, which lifts the degeneracy of the t symmetry non-relativistic single-group MOs (the symmetry labels of the relativistic energy levels belong to the octahedral double-point group, O_h*).

The experimentally determined[77] electronic transition energies are given in italics on the relativistic MO diagram. Comparison of the calculated and experimental data reveals that the relativistic calculations do an excellent job of reproducing experiment. (The lowest energy $e_{5/2}^- \longrightarrow g_{3/2}^-$ transition was not detected experimentally; data were not acquired below 5000 cm^{-1}.) It is also clear that the non-relativistic calculations show very poor agreement with experiment, both qualitatively (they predict too few transitions) and quantitatively. Analogous calculations on other octahedral $5f^1$ complexes[76] (PaX_6^{2-}, X = halide; UX_6^-, X = Cl or Br; NpF_6) give similar agreement with experiment.

It is worth emphasising that the factors that complicate transition-metal optical spectra (electron–electron repulsions, Jahn–Teller splitting, vibronic coupling, *etc.*) are no less com-

Table 5 Ionisation energies and band assignments of the valence photoelectron spectrum of OsO_4. Ionisation energy data from ref. 84

Band	Ionisation energy/eV	Non-relativistic ion state	Associated non-relativistic MO [a]	Relativistic ion state	Associated relativistic MO [b]
A	12.35	$^2T_1$	$1t_1$	$G_{3/2} + E_{1/2}$	$4g_{3/2} + 2e_{1/2}$
B	13.14	$^2T_2$	$3t_2$	$G_{3/2}$	$3g_{3/2}$
C	13.54	$^2T_2$	$3t_2$	$E_{5/2}$	$2e_{5/2}$
D	14.66	$^2A_1$	$2a_1$	$E_{1/2}$	$1e_{1/2}$
E	16.4, 16.8	$^2T_2 + {}^2E$	$2t_2 + 1e$	$E_{5/2} + G_{3/2} + G_{3/2}$	$1e_{5/2} + 2g_{3/2} + 1g_{3/2}$

[a] Orbital numbering scheme from Figs. 7 and 9. [b] Orbital numbering scheme from Fig. 9.

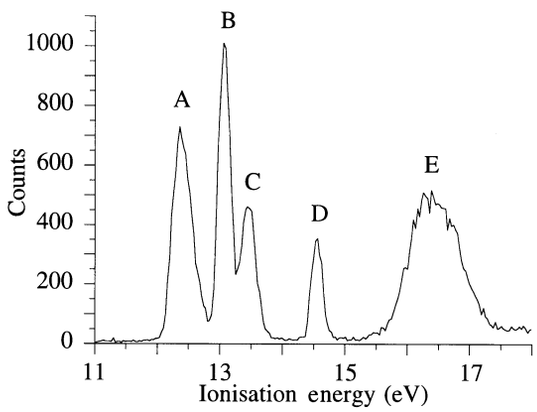

Fig. 8 Valence photoelectron spectrum of OsO_4, acquired with synchrotron radiation at 39 eV. Data from refs. 84 and 90

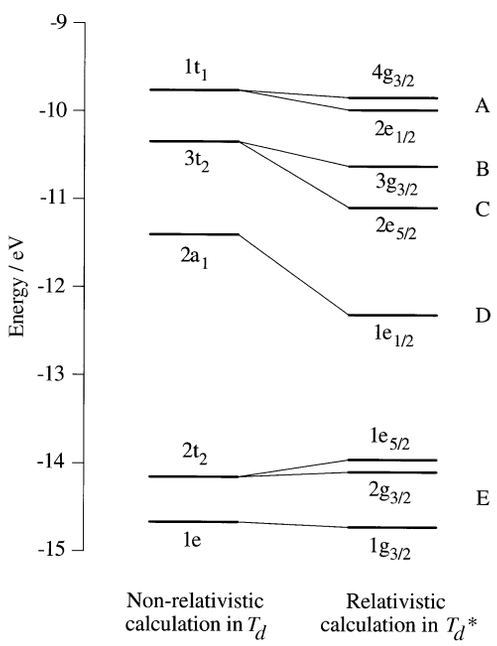

Fig. 9 Calculated non-relativistic and relativistic molecular orbital energy levels of OsO_4. Letters on the right-hand side refer to the bands in the photoelectron spectrum (Fig. 8) that the orbitals give rise to. Relativistic molecular orbital symmetry labels belong to the T_d* double-point group. Data from ref. 89

mon in actinide systems. Thus relativity exacerbates an already complex situation; separating the effects of relativity from those of interelectronic repulsion, Jahn–Teller distortion and metal–ligand bond vibrations is part of the challenge of heavy-element electronic spectroscopy.

Photoelectron spectrum of OsO_4

Tetrahedral co-ordination is one of the geometries central to inorganic chemistry, and a thorough appreciation of the electronic structure of tetrahedral molecules is of key importance in understanding a wide range of chemical systems. Osmium tetraoxide is a classic example of a tetrahedral molecule, and there have been extensive photoelectron (PE) spectroscopic investigations of its electronic structure,[78–84] as well as numerous calculational studies.[84–89] The assignment of its PE spectrum has been the subject of debate for over 20 years, but I now believe that this has finally been resolved, with relativistic effects playing a central role.

A qualitative non-relativistic valence MO energy-level scheme for OsO_4 is given in Fig. 7. The $1a_1$ and $1t_2$ are essentially oxygen 2s orbitals. Of the remaining occupied levels, the $2t_2$ and $2a_1$ are traditionally associated with Os–O σ bonding and the 1e and $3t_2$ with Os–O π bonding, although there is strictly no σ/π separability in t_2 MOs in T_d symmetry. The $1t_1$ HOMO is metal–ligand non-bonding.

Five primary ion states are therefore expected to occur in the PE spectrum of OsO_4 in the valence ionisation energy (IE) region, a $^2A_1$, a ^2E, a $^2T_1$ and two $^2T_2$. These result from ionisation of the 1e–$1t_1$ MOs. The PE spectrum of OsO_4 is shown in Fig. 8, and there are indeed five bands, labelled A–E. However, there is not a simple one to one correspondence between the PE bands and the primary ion states. The most likely assignment is given in Table 5, from which it may be seen that band E contains the ^2E and $^2T_2$ (from the $2t_2$ MO) primary ion states. Thus bands A–D are the result of only three primary ion states, with B and C being the spin–orbit components of the $^2T_2$ ($3t_2$) state.

Space does not permit me to go into the reasons for this assignment; suffice it to say that there is extensive experimental and theoretical evidence to support it. The origin of the spin–orbit splitting of bands B and C is, however, of particular interest. The puzzle is this: as the $3t_2$ MO is largely oxygen 2p-based, why is the spin–orbit splitting so large (0.40 eV)? Clearly spin–orbit splitting of this magnitude must originate from the metal, but it cannot be due to a 5d contribution to the $3t_2$ MO as the relative ordering of the $G_{3/2}$ and $E_{5/2}$ ion states is contrary to that expected for splitting of a t_2 MO with d character.[84] The only possibility is an osmium p AO contribution, presumably the 6p valence AO. It was felt, however, that the 6p character of the $3t_2$ MO was too small to produce the required spin–orbit splitting.[84]

Relativistic DFT was recently employed[89] in an attempt to resolve this dilemma, and the results are presented pictorially in Fig. 9. It was found that bands B and C indeed stem from the same $^2T_2$ primary ion state, with the osmium p AO content in the associated $3t_2$ MO the cause of the spin–orbit splitting. Interestingly this p content is not purely 6p, but also includes a very small 5p contribution (<1%). Such a small AO contribution to a MO would normally be disregarded, but in this case the magnitude of the spin–orbit coupling in the osmium semi-core 5p AO is so great (the osmium 5p AO spin–orbit splitting is 12.8 eV[33]) that even a tiny contribution to the non-relativistic $3t_2$ orbital affects the separation of the relativistic $2e_{5/2}$ and $3g_{3/2}$ levels. The conclusion was that the 6p AO content of the $3t_2$ MO is responsible for approximately 2/3 of the spin–orbit splitting, with the 5p contribution accounting for the remainder.

Conclusion

I hope that the topics addressed in this contribution have given the reader some insight into the role of relativity in chemistry, and have shown that Dirac's initial conclusion as to the chemical significance of relativity was some way off the mark. I have no doubt that the effects of relativity in heavy-element chemistry will continue to be a fruitful area of research, particularly for the computational quantum chemist. Recent evidence[91] that the lifetimes of superheavy elements with $Z > 109$ may be much higher than previously anticipated may well take investigators further into the largely unexplored area of transactinide chemistry. These elements are expected to exhibit relativistic effects to an even greater extent than do the third-row transition metals and actinides. Indeed it was recently predicted[32] that the transactinide elements should have an *actinide* contraction so great that element 111 (which lies below gold) has a smaller atomic radius than any of its lighter Group 11 congeners! Furthermore this actinide contraction, unlike the lanthanide equivalent, is found to be almost exclusively a relativistic effect.

Acknowledgements

I would like to thank the facilitators of this article, Professor Jim Turner, Dr. Philip Mountford and Dr. Jennifer Green. I am also grateful to the reviewers for their helpful comments and suggestions.

References

1 P. A. M. Dirac, *Proc. R. Soc. London, Ser. A*, 1928, **117**, 610.
2 P. A. M. Dirac, *Proc. R. Soc., London Ser. A*, 1928, **118**, 351.
3 P. A. M. Dirac, *Proc. R. Soc., London Ser. A*, 1929, **123**, 714.
4 P. Pyykkö, *Chem. Rev.*, 1988, **88**, 563.
5 K. S. Pitzer, *Acc. Chem. Res.*, 1979, **12**, 271.
6 P. Pyykkö and J. P. Desclaux, *Acc. Chem. Res.*, 1979, **12**, 276.
7 K. Balasubramanian and K. S. Pitzer, *Adv. Chem. Phys.*, 1987, **67**, 287.
8 M. Pepper and B. E. Bursten, *Chem. Rev.*, 1991, **91**, 719.
9 P. A. M. Dirac, *The principles of quantum mechanics*, 4th edn., Oxford Univesity Press, 1958.
10 M. Mizushima, *Quantum Mechanics of Atomic Spectra and Atomic Structure*, Benjamin, New York, 1970.
11 A. Rubinowicz, *Quantum Mechanics*, Elsevier, Amsterdam, 1968.
12 (*a*) C. D. Anderson, *Phys. Rev.*, 1933, **43**, 491; (*b*) W. H. E. Schwarz, E. M. van Wezenbeek, E. J. Baerends and J. G. Snijders, *J. Phys. B*, 1989, **22**, 1515.
13 P. W. Atkins, *Molecular Quantum Mechanics*, 2nd edn., Oxford Univesity Press, 1983.
14 C. E. Moore, *At. Energy Levels, NSRDS-NBS 35*, 1971, **1**.
15 F. A. Cotton, *Chemical Applications of Group Theory*, 3rd edn., Wiley-Interscience, New York, 1991.
16 J. A. Salthouse and M. J. Ware, *Point group character tables and related data*, Cambridge University Press, London, 1972.
17 L. L. Lohr and P. Pyykkö, *Chem. Phys. Lett.*, 1979, **62**, 333.
18 D. D. Koelling and B. N. Harmon, *J. Phys. C*, 1977, **10**, 3107.
19 J. H. Wood and A. M. Boring, *Phys. Rev. B*, 1978, **18**, 2701.
20 T. Ziegler, V. Tschinke, E. J. Baerends, J. G. Snijders and W. Ravenek, *J. Phys. Chem.*, 1989, **93**, 3050.
21 L. R. Kahn, P. J. Hay and R. D. Cowan, *J. Chem. Phys.*, 1978, **68**, 2386.
22 A. Rosén and D. E. Ellis, *J. Chem. Phys.*, 1975, **62**, 3039.
23 D. E. Ellis, *J. Phys. B*, 1977, **10**, 1.
24 Y. S. Lee, W. C. Ermler and K. S. Pitzer, *J. Chem. Phys.*, 1977, **67**, 5861.
25 J. A. Moriarty, *Phys. Lett. A*, 1988, **131**, 46.
26 M. Kaupp, M. Dolg, H. Stoll and H. G. VonSchnering, *Inorg. Chem.*, 1994, **33**, 2122.
27 M. Kaupp and H. G. VonSchnering, *Inorg. Chem.*, 1994, **33**, 2555.
28 M. Kaupp and H. G. VonSchnering, *Inorg. Chem.*, 1994, **33**, 4718.
29 A. F. Wells, *Structural Inorganic Chemistry*, 5th edn., Clarendon Press, Oxford, 1984.
30 A. Bayler, A. Schier, G. A. Bowmaker and H. Schmidbaur, *J. Am. Chem. Soc.*, 1996, **118**, 7006.
31 P. S. Bagus, Y. S. Lee and K. S. Pitzer, *Chem. Phys. Lett.*, 1975, **33**, 408.
32 M. Seth, M. Dolg, P. Fulde and P. Schwerdtfeger, *J. Am. Chem. Soc.*, 1995, **117**, 6597.
33 J. P. Desclaux, *At. Data Nucl. Data Tables*, 1973, **12**, 311.
34 J. Emsley, *The Elements*, 2nd edn., Oxford Univesity Press, 1991.
35 P. Pyykkö, *Adv. Quantum Chem.*, 1978, **11**, 353.
36 N. E. Christensen and B. O. Seraphin, *Phys. Rev. B*, 1971, **4**, 3321.
37 C. Heinemann, R. H. Hertwig, R. Wesendrup, W. Koch and H. Schwarz, *J. Am. Chem. Soc.*, 1995, **117**, 495.
38 T. Bastug, D. Heinemann, W. D. Sepp, D. Kolb and B. Fricke, *Chem. Phys. Lett.*, 1993, **211**, 119.
39 I. Antes and G. Frenking, *Organometallics*, 1995, **14**, 4263.
40 A. Szabo and N. S. Ostlund, *Modern Quantum Chemistry*, McGraw-Hill, New York, 1989.
41 T. Ziegler, J. G. Snijders and E. J. Baerends, *Chem. Phys. Lett.*, 1980, **75**, 1.
42 J. G. Snijders and P. Pyykkö, *Chem. Phys. Lett.*, 1980, **75**, 5.
43 T. Ziegler, J. G. Snijders and E. J. Baerends, *J. Chem. Phys.*, 1981, **74**, 1271.
44 H. Schmidbaur, F. Scherbaum, B. Huber and G. Müller, *Angew. Chem., Int. Ed. Engl.*, 1988, **27**, 419.
45 H. Schmidbaur, *Gold Bull.*, 1990, **23**, 1.
46 A. Görling, N. Rösch, D. E. Ellis and H. Schmidbaur, *Inorg. Chem.*, 1991, **30**, 3986.
47 J. Li and P. Pyykkö, *Chem. Phys. Lett.*, 1992, **197**, 586.
48 P. Pyykkö, J. Li and N. Runeberg, *Chem. Phys. Lett.*, 1994, **218**, 133.
49 O. D. Häberlein, H. Schmidbaur and N. Rösch, *J. Am. Chem. Soc.*, 1994, **116**, 8241.
50 J. W. Lauher and R. Hoffmann, *J. Am. Chem. Soc.*, 1976, **98**, 1729.
51 K. Tatsumi and A. Nakamura, *J. Organomet. Chem.*, 1984, **272**, 141.
52 B. E. Bursten and R. J. Strittmatter, *J. Am. Chem. Soc.*, 1987, **109**, 6606.
53 B. E. Bursten, L. F. Rhodes and R. J. Strittmatter, *J. Am. Chem. Soc.*, 1989, **111**, 2756.
54 B. E. Bursten, L. F. Rhodes and R. J. Strittmatter, *J. Am. Chem. Soc.*, 1989, **111**, 2758.
55 B. E. Bursten, L. F. Rhodes and R. J. Strittmater, *J. Less-Common Met.*, 1989, **149**, 207.
56 R. J. Strittmatter and B. E. Bursten, *J. Am. Chem. Soc.*, 1991, **113**, 552.
57 L. J. Nugent, P. G. Laubereau, G. K. Werner and K. L. van der Sluis, *J. Organomet. Chem.*, 1971, **27**, 365.
58 P. N. Hazin, J. W. Bruno and H. G. Brittain, *Organometallics*, 1987, **6**, 913.
59 N. Kaltsoyannis and B. E. Bursten, *J. Organomet. Chem.*, 1996, in the press.
60 S. Dibella, A. Gulino, G. Lanza, I. Fragala, D. Stern and T. J. Marks, *Organometallics*, 1994, **13**, 3810.
61 R. J. Strittmatter, Ph.D. Dissertation, The Ohio State University, 1990.
62 W. K. Kot, G. V. Shalimoff, N. M. Edelstein, M. A. Edelman and M. F. Lappert, *J. Am. Chem. Soc.*, 1988, **110**, 986.
63 W. K. Kot, Ph.D. Thesis, Lawrence Berkeley Laboratory, University of California, 1991.
64 P. Pyykkö, L. J. Laakkonen and K. Tatsumi, *Inorg. Chem.*, 1989, **28**, 1801.
65 P. M. Boerrigter, E. J. Baerends and J. G. Snijders, *Chem. Phys.*, 1988, **122**, 357.
66 M. J. S. Dewar, *Bull. Soc. Chim. Fr.*, 1951, **18**, C71.
67 J. Chatt and L. A. Duncanson, *J. Chem. Soc.*, 1953, 2939.
68 J. Li, G. Schreckenbach and T. Ziegler, *J. Am. Chem. Soc.*, 1995, **117**, 486.
69 S. Dapprich and G. Frenking, *J. Phys. Chem.*, 1995, **99**, 9352.
70 J. Li, G. Schreckenbach and T. Ziegler, *Inorg. Chem.*, 1995, **34**, 3245.
71 S. X. Xiao, W. C. Trogler, D. E. Ellis and Z. Berkovitch-Yellin, *J. Am. Chem. Soc.*, 1983, **105**, 7033.
72 J. B. Brennan, J. C. Green, C. M. Redfern and M. A. MacDonald, *J. Chem. Soc., Dalton Trans.*, 1990, 1907.
73 J. C. Green, N. Kaltsoyannis, M. A. MacDonald and K. H. Sze, *J. Chem. Soc., Dalton Trans.*, 1991, 2371.
74 P. Fantucci, S. Polezzo, M. Sironi and A. Bencini, *J. Chem. Soc., Dalton Trans.*, 1995, 4121.
75 H. Hartman, H. L. Schläfer and K. H. Hansen, *Z. Anorg. Allg. Chem.*, 1956, **284**, 153.
76 N. Kaltsoyannis and B. E. Bursten, *Inorg. Chem.*, 1995, **34**, 2735.
77 J. L. Ryan, *J. Inorg. Nucl. Chem.*, 1971, **33**, 153.
78 E. Diemann and A. Müller, *Chem. Phys. Lett.*, 1973, **19**, 538.
79 S. Foster, S. Phelps, L. C. Cusachs and S. P. McGlynn, *J. Am. Chem. Soc.*, 1973, **95**, 5521.
80 S. Evans, A. Hamnett and A. F. Orchard, *J. Am. Chem. Soc.*, 1974, **96**, 6621.

81 F. Burroughs, S. Evans, A. Hamnett, A. F. Orchard and N. V. Richardson, *J. Chem. Soc., Faraday Trans. 2*, 1974, 1895.
82 R. G. Egdell, D. Phil. Thesis, Oxford University, 1977.
83 J. C. Green, N. Kaltsoyannis, M. A. MacDonald and K. H. Sze, *Chem. Phys. Lett.*, 1990, **175**, 359.
84 J. C. Green, M. F. Guest, I. H. Hillier, S. A. Jarrett-Sprague, N. Kaltsoyannis, M. A. MacDonald and K. H. Sze, *Inorg. Chem.*, 1992, **31**, 1588.
85 A. Rauk, T. Ziegler and D. E. Ellis, *Theor. Chim. Acta*, 1974, **34**, 49.
86 J. Weber, *Chem. Phys. Lett.*, 1977, **45**, 261.
87 R. Arratia-Pérez, *Chem. Phys. Lett.*, 1993, **204**, 409.
88 P. Pyykkö, J. Li, T. Bastug, B. Fricke and D. Kolb, *Inorg. Chem.*, 1993, **32**, 1525.
89 B. E. Bursten, J. C. Green and N. Kaltsoyannis, *Inorg. Chem.*, 1994, **33**, 2315.
90 N. Kaltsoyannis, D. Phil. Thesis, Oxford University, 1992.
91 Y. A. Lazarev, Y. V. Lobonov, Y. T. Oganessian, V. K. Utyonkov, F. S. Abdullin, G. V. Buklanov, B. N. Gikal, S. Iliev, A. N. Mezentsev, A. N. Polyakov, I. M. Sedykh, I. V. Shirokovsky, V. G. Subbotin, A. M. Sukhov, Y. S. Tsyganov, V. E. Zhuchko, R. W. Lougheed, K. J. Moody, J. F. Wild, E. K. Hulet and J. H. McQuaid, *Phys. Rev. Lett.*, 1994, **73**, 624.

Received 5*th August* 1996; *Paper* 6/05473K